atmosphere

MDPI

Article

Contribution of Climate Change and Human Activities to Runoff and Sediment Discharge Changes Based on Budyko Theory and Water–Sediment Relationships during 1960–2019 in the Taohe River Basin, China

Yali Ma, Dongyuan Sun *, Zuirong Niu and Xingfan Wang

College of Water Conservancy and Hydropower Engineering, Gansu Agricultural University, Lanzhou 730070, China
* Correspondence: sundy@gsau.edu.cn

Abstract: Variations in runoff and sediment discharge are important characteristic variables for revealing the coupled effects of climate change (including both the natural variability of climate and anthropogenic climate change) and human activities (including soil and water conservation measures, land use changes, and hydraulic engineering construction). Based on the meteorological data from 19 meteorological stations and the hydrological data from the watershed control station of Hongqi Station, the temporal and spatial evolution of runoff and sediment discharge and the water–sand relationship were analyzed, and the response mechanisms of runoff and sediment discharge changes were clarified using Mikhail Budyko's theory and other qualitative and quantitative methods. The results determined that: (1) The runoff and sediment discharge showed significant downward trends, with linear change rates of -0.28×10^8 m^3/a and -46.10×10^4 t/a, respectively. The change points of the runoff and sediment discharge occurred in 1987 and 1996, respectively. (2) The spatial distribution of water and sediment was different, and the upper and middle reaches produced water, while the downstream produced sediment. (3) Comparing potential evapotranspiration and rainfall based on Budyko theory and the regression relationship, runoff is more closely related to rainfall, and runoff changes are more affected by it. The change in sediment discharge is most closely related to sediment concentration, followed by rainfall and potential evaporation. (4) The contribution rates of runoff and sediment discharge changes influenced by climate change were 24% and 3%, respectively, and the contribution rates by human activities were 76% and 97%, respectively. Human activities, including soil and water conservation measures, land use changes, and hydraulic engineering construction were the main influencing factors, and the impacts of human activities increased from 1960 to 2019. The research results are of great significance for erosion control and ecological restoration in the Tao River Basin under the conditions of the changing environment.

Keywords: contribution; Budyko theory; sediment discharge; runoff; water–sediment relationship; the Taohe River Basin

check for updates

Citation: Ma, Y.; Sun, D.; Niu, Z.; Wang, X. Contribution of Climate Change and Human Activities to Runoff and Sediment Discharge Changes Based on Budyko Theory and Water–Sediment Relationships during 1960–2019 in the Taohe River Basin, China. *Atmosphere* **2023**, *14*, 1144. https://doi.org/10.3390/atmos14071144

Academic Editors: Ognjen Bonacci and Dae Il Jeong

Received: 22 May 2023
Revised: 8 July 2023
Accepted: 11 July 2023
Published: 13 July 2023

Copyright: © 2023 by the authors. Licensee MDPI, Basel, Switzerland. This article is an open access article distributed under the terms and conditions of the Creative Commons Attribution (CC BY) license (https://creativecommons.org/licenses/by/4.0/).

1. Introduction

Runoff and sediment discharge not only directly represent the hydrological characteristics of river runoff, but also indirectly reflect regional ecological environmental changes and soil and water loss. The Yellow River is one of the world's largest sediment-discharge rivers. Runoff and sediment are an important basis for soil and water loss control in the Yellow River Basin. Since the 1950s, runoff and sediment discharge of the Yellow River have been sharply reduced, at a rate exceeding 50% [1–3], and the frequency and severity of extreme hydrological events have increased [4]. The decrease in sediment discharge causes the retreat of the estuarine delta and the reduction of nutrient transport, which seriously threatens the health of the ecosystem in the coastal region [5]. Therefore, coordinating

and maintaining a good water–sediment relationship is of great significance to sustainable water use and sediment regulation [6]. Factors affecting runoff and sediment discharge include climate change (variations in meteorological elements), geographical conditions, and human activities (soil and water conservation measures, land use changes, and hydraulic engineering construction). In the 100-year time scale, climate change and human activities are the two main influencing aspects [7]. The combined effects of the two factors cause changes in the spatial and temporal pattern of the terrestrial hydrological cycle [8,9], and the degree of influence varies with different geographical locations and time periods [10,11]. Changes in climate factors such as temperature and precipitation directly affect the regional water cycle [12] and cause changes in hydrological factors such as runoff and sediment [13]. The Yellow River flows through the Loess Plateau region, which has a fragile ecological environment and has experienced serious soil and water loss. To improve the serious water and soil erosion situation, a series of comprehensive water and soil erosion management measures at the catchment scale have been carried out. Human intervention has curbed soil and water loss in the basin to a certain extent, and has promoted the change in runoff and sediment discharge [14]. Therefore, the dual coupling effects of climate change and human activities promote changes in water and sediment in the basin, making the relationship between water and sediment more complex [15,16].

In recent years, due to the global climate evolution and the implementation of policies for returning farmland to forest (grassland) on the Loess Plateau, the amount of runoff and sediment in each branch of the Yellow River has significantly decreased, while the vegetation coverage, such as woodlands and grasslands, has significantly increased, resulting in significant changes in the regional hydrological situation and ecological conditions [17]. Among climate factors, precipitation has a significant impact on runoff and is the driving force of hydraulic erosion, which in turn has an impact on sediment discharge [18]. Soil and water conservation measures as a result of human activity have a great effect on the reduction of runoff and sediment discharge [3,17,19], and there is a close relationship between rainfall, runoff, and sediment discharge [3,19]. It is of great significance for water resource management and basin ecological construction to study the variation characteristics of runoff and sediment discharge, the correlation among influencing factors, and the response mechanisms. Wang, S., et al. [5] found that the sharp decrease in sediment after 1979 was mainly caused by the decrease in water yield, and 76% of the decrease in water yield was caused by changes in underlying surface conditions such as terracing, the construction of check-dams and reservoirs, and large-scale vegetation restoration projects. Keo, S. et al. [20] analyzed the changes in rainfall erosivity in the Loess Plateau over the last 50 years and found that extreme rainfall was the main factor affecting soil erosion, but the annual rainfall erosivity showed a significant decreasing trend in the Loess Plateau. The existing studies mainly focus on the characteristics of runoff or sediment change at one or more hydrological stations and mostly adopt quantitative methods, such as the elastic coefficient method and hydrological modeling method for runoff attribution analysis [10,21]. The main methods used to isolate the different factors influencing runoff variability are physically based hydrological models, empirical statistical methods, and conceptual methods [22]. Xu, R. et al. [23] comprehensively reviewed four commonly used quantitative methods: the SWAT model, the Budyko-based method, and two empirical methods, and pointed out the advantages and limitations of each method. The Budyko-based method has been successfully used to quantitatively assess the contribution of climate change and human activities to runoff changes [24,25]. Li, C. et al. [26] used the Budyko hypothesis to analyze the reasons for the decreasing trend of streamflow from 1960 to 2015 in the Yarlung Zangbo River. Sun, X. et al. [27] analyzed the attribution of extreme drought events and the associated physical drivers in southwest China based on the Budyko framework. However, applications that combine qualitative and quantitative attribution analyses of runoff and sediment evolution are lacking.

Therefore, an analytical method combining traditional qualitative analysis with a quantitative calculation based on Budyko theory and water–sediment relationships was built. The objectives of this study were: (1) from the perspective of qualitative and quantitative analysis, to build an analytical method that combines traditional mathematical and statistical qualitative analysis with a quantitative calculation based on Budyko theory and water–sediment relationships; (2) to reveal the spatiotemporal evolution of runoff and sediment discharge and driving variables; (3) to explore the qualitative and quantitative relationships between the changes in runoff and sediment discharge and the driving variables, and to clarify the response mechanism to runoff and sediment discharge changes in the Taohe River Basin. The research results are of great significance for the prevention and control of soil erosion and the promotion of sustainable water use in the basin.

2. Materials and Methods

2.1. Study Area

The Taohe River is a first-level tributary of the upper reaches of the Yellow River at the right bank, located in the south of Gansu Province, with the geographical coordinates of 101°36′~104°20′ E, 34°06′~36°01′ N. Originating from the Xiqingshan Mountain, the Taohe River flows into the Liujiaxia Reservoir in the main stream of the Yellow River, with a total length of 673 km and a watershed area of 25,527 km^2. The Taohe River Basin spans three geomorphic units. The grasslands are widely spread in the upper reaches, where the terrain is relatively flat and the vegetation is good, with an altitude above 3000 m. The middle reaches are alpine canyon areas, where the water energy resources are abundant and the forest grassland is covered, with an altitude above 2000 m. The lower reaches are loess hilly regions, where the terrain is fragmented, vegetation coverage is poor, and soil erosion is serious [28]. The sources of water and sediment are different, with the middle and upper reaches of the basin producing water, and the lower reaches producing sand. The Taohe River Basin, in Gansu Province, is abundant in water and has a large runoff. The upper and middle reaches of the basin are cold and humid, while the lower reaches are warm and arid. The average annual temperature increases from 1 °C in the upper reaches to 9 °C in the lower reaches, and the average annual precipitation decreases from 650 mm in the upper reaches to 300 mm in the lower reaches [29].

2.2. Data

The daily precipitation data from 1960–2019 of 19 meteorological stations in and around the Taohe River Basin were obtained from the China Meteorological Data Network (http://data.cma.cn, accessed on 12 June 2022). The rainfall, rainfall erosivity [30], and potential evapotranspiration [31] of the basin were calculated using the Thiessen polygon weighted method based on the data from the 19 meteorological stations. The monthly runoff and sediment discharge data from 1956 to 2019 of a control station in the lower reaches of the Taohe River Basin, namely Hongqi Hydrological Station, were adopted, and the data were extracted from the hydrological yearbook. The location and distribution of hydrometeorological stations in the Taohe River Basin are shown in Figure 1.

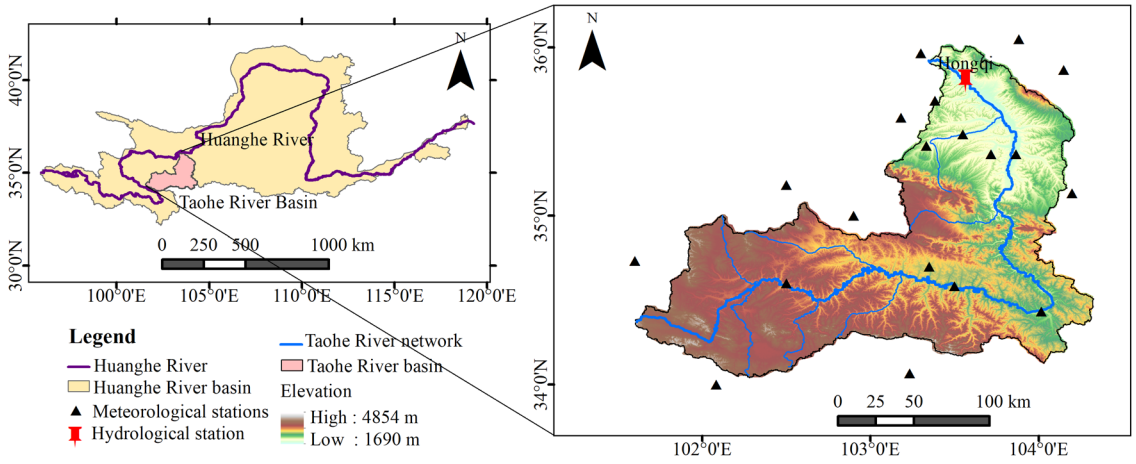

Figure 1. Distribution of hydrometeorological stations in Taohe River Basin.

2.3. Methodology

2.3.1. Calculation of Rainfall Erosivity

The calculation method of Richardson's daily rainfall erosivity, as improved by Zhang Wenbo et al. [30], is used to calculate rainfall erosivity based on daily rainfall data, and is suitable for the Loess Plateau [32]. The formula is as follows:

$$\begin{aligned} R &= \sum_{n=1}^{24} R_{\text{half a month}} \\ R_{\text{half a month}} &= \alpha \sum_{k=1}^{m} P_k^{\beta} \\ &\begin{cases} \alpha = 21.586\beta^{-7.1891} \\ \beta = 0.8363 + \frac{18.144}{P_{d12}} + \frac{24.455}{P_{y12}} \end{cases} \end{aligned} \quad (1)$$

where k is the time of erosive rainfall within half a month, d; m is the time within half a month, d; P_k is ≥12 mm daily rainfall on the k day within half a month, mm; R and $R_{\text{half a month}}$ are the rainfall erosivity of a year and half a month, respectively, MJ·mm·(hm^2·h·a)$^{-1}$; α, β are model parameters; P_{d12} is ≥12 mm daily average rainfall, mm; and P_{y12} is ≥12 mm annual average daily rainfall, mm. According to the standard of soil and water conservation special census of China's first national water conservancy survey, 12.0 mm was taken as the standard of erosive rainfall. The rainfall erosivity was calculated at stations, and the rainfall erosivity of the basin was obtained by the Thiessen polygon weighted method based on station rainfall erosivity.

2.3.2. Calculation of Potential Evapotranspiration

The Penman–Monteith formula [31] modified by the Food and Agriculture Organization of the United Nations (FAO) in 1998 was adopted to calculate the potential evapotranspiration at each meteorological station. The P-M method was based on energy balance and aerodynamic principles and comprehensively considered the influence of temperature, radiation, wind speed, humidity, and geographical location (altitude and latitude). It has been shown to have high calculation accuracy in different regions and under different climatic conditions [33,34]. Its formula is as follows [31]:

$$ET_0 = \frac{0.408\Delta(R_n - G) + \gamma\frac{900}{T+273}u_2(e_s - e_a)}{\Delta + \gamma(1 + 0.34u_2)} \quad (2)$$

where ET_0 is the daily potential evapotranspiration (mm·d^{-1}); Δ is the slope vapor pressure curve (kPa·°C^{-1}); R_n is the net solar radiation (MJ·m^{-2}·d^{-1}); and G is the soil heat flux (MJ·m^{-2}·d^{-1}), which is ignored on the daily scale and denoted as 0. γ is the psychrometric

constant (kPa·°C^{-1}); u_2 is the wind speed at a height of 2 m (m·s^{-1}); T is the average temperature (°C); e_s is the saturation vapor pressure (kPa); e_a is the actual vapor pressure (kPa); and ($e_s - e_a$) is the saturation vapor pressure deficit (kPa).

2.3.3. Contribution to Runoff Change Based on Water Balance and the Budyko Hypothesis

Budyko assumed that the energy balance assumptions apply to the global flow of green water, i.e., negligible changes in subsurface water storage and negligible net heat transfer between the surface and the vadose zone [35,36]. Under these two assumptions, the long-term average annual water and energy balance at the catchment scale can be expressed as:

$$Q = P - ET_a \tag{3}$$

$$R_n = L{\cdot}ET_a + H \tag{4}$$

where ETa is the actual evapotranspiration (mm/a), P is the precipitation (mm/a), and Q is the runoff (mm/a). R_n is the net solar radiation (MJ·m^{-2}·d^{-1}); L·ETa is the latent heat flux (MJ·m^{-2}·d^{-1}), and H is the sensible heat flux (MJ·m^{-2}·d^{-1}).

Based on the Budyko hypothesis theory, the actual evapotranspiration of a specific watershed on a multi-year scale is a function of the two climate variables, P and ET_0, which can be expressed as $ET_a = f(P, ET_0)$ [36].

Hankey and Stanley [37] have proved that the property of homogeneity, as expressed in Equation (5), is mathematically equivalent to the representation:

$$ET_a = P{\cdot}f\left(\frac{ET_0}{P}\right) \tag{5}$$

The Choudhury–Yang [38,39] model based on the Budyko framework can be expressed as follows:

$$ET_a = P{\cdot}f\left(\frac{ET_0}{P}\right) = P\frac{ET_0}{\left(P^n + {ET_0}^n\right)^{1/n}} \tag{6}$$

Equation (6) is substituted into Equation (3). Since runoff is a function of rainfall P, potential evapotranspiration ET_0, and watershed catchment characteristics n, it can be denoted as $Q = f(P, ET_0, n)$, where P, ET_0, and n are independent variables and Q is the dependent variable based on Equations (3) and (6). The total differential equation of Q is shown in Equation (7):

$$dQ = \frac{\partial Q}{\partial P}dP + \frac{\partial Q}{\partial ET_0}dET_0 + \frac{\partial Q}{\partial n}dn \tag{7}$$

According to the definition of the elastic coefficient by Schaake [40], the rainfall elasticity coefficient ε_P, the potential evapotranspiration elasticity coefficient ε_{ET0}, and the elasticity coefficient of watershed characteristic parameters ε_n are expressed as $\varepsilon_P = \frac{\partial Q/Q}{\partial P/P}$, $\varepsilon_{ET_0} = \frac{\partial Q/Q}{\partial ET_0/ET_0}$, and $\varepsilon_n = \frac{\partial Q/Q}{\partial n/n}$, respectively. Equation (7) is transformed into Equation (8):

$$\frac{dQ}{Q} = \varepsilon_P\frac{dP}{P} + \varepsilon_{ET_0}\frac{dET_0}{ET_0} + \varepsilon_n\frac{dn}{n} \tag{8}$$

where Q is runoff, P is precipitation, ET_0 is potential evapotranspiration, and n is watershed catchment characteristics. The quantitative response of runoff to climate change and human activities can be expressed as:

$$\Delta Q_P = \varepsilon_P\frac{\Delta P}{P}Q,\ \Delta Q_{ET_0} = \varepsilon_{E_0}\frac{\Delta ET_0}{ET_0}Q,\ \Delta Q_n = \varepsilon_n\frac{\Delta n}{n}Q \tag{9}$$

where ΔP, ΔET_0, and Δn are the changes in precipitation, potential evapotranspiration, and landscape, respectively.

The contribution of climate change (δ_C) and human activities (δ_H) can be expressed as:

$$\delta_C = \frac{\Delta Q_P + \Delta Q_{ET_0}}{\Delta Q} \times 100\%,\ \delta_H = \frac{\Delta Q_n}{\Delta Q} \times 100\% \tag{10}$$

2.3.4. Contribution to Sediment Discharge Change Based on the Budyko Hypothesis and Water–Sediment Relationships

Based on the Budyko framework, the principle of water balance [36], and the water–sediment relationship expressed in Equation (11), the influences of climate change and human activities on sediment discharge changes are determined. The differential formula of sediment discharge is defined as follows [41]:

$$dS = \frac{\partial S}{\partial Q} dQ + \frac{\partial S}{\partial C} dC \tag{11}$$

where S is the sediment discharge ($t/(km^2 \cdot a)$), Q is the runoff (mm), and C is the concentration of suspended sediment (kg/m^3), which is obtained from S/Q at the site.

Equation (8) is substituted into Equation (11). Since sediment discharge is a function of rainfall P, potential evapotranspiration ET_0, catchment characteristics n, and sediment concentration C, it can be denoted as $S = f(P, ET_0, n, C)$, and the sediment discharge S differential Equation (12) can be obtained:

$$\frac{dS}{S} = \frac{\partial S/S}{\partial Q/Q}\left(\frac{\partial Q/Q}{\partial P/P}\frac{dP}{P} + \frac{\partial Q/Q}{\partial ET_0/ET_0}\frac{dET_0}{ET_0} + \frac{\partial Q/Q}{\partial n/n}\frac{dn}{n}\right) + \frac{\partial S/S}{\partial C/C}\frac{dC}{C} \tag{12}$$

The units of the numerator and denominator are the same, and by dividing, each part of the formula is dimensionless and unitless. Where $\eta_Q = \frac{\partial S/S}{\partial Q/Q}$, $\eta_{mC} = \frac{\partial S/S}{\partial C/C}$, the relationship formula is deduced and established between the runoff elasticity coefficient and the sediment discharge elasticity coefficient:

$$\eta_P = \eta_Q \times \varepsilon_P,\ \eta_{ET_0} = \eta_Q \times \varepsilon_{ET_0},\ \eta_n = \eta_Q \times \varepsilon_n \tag{13}$$

The quantitative response of sediment discharge to rainfall P, potential evapotranspiration ET_0, catchment characteristics n, and sediment concentration C can be expressed as:

$$\begin{aligned} \Delta S_P &= \eta_P \tfrac{\Delta P}{P} S,\ \Delta S_{ET_0} = \eta_{ET_0} \tfrac{\Delta ET_0}{ET_0} S \\ \Delta S_n &= \eta_n \tfrac{\Delta n}{n} S,\ \Delta S_{mC} = \eta_{mC} \tfrac{\Delta C}{C} S \end{aligned} \tag{14}$$

where ΔS_P, ΔS_{ET_0}, ΔS_n, and ΔS_{mC} are the change amount of sediment discharge influenced by precipitation, potential evapotranspiration, watershed catchment characteristics, and sediment concentration, respectively. The contribution of climate change (δ_C') and human activities (δ_H') can be expressed as:

$$\delta'_C = \frac{\Delta S_P + \Delta S_{ET_0}}{\Delta S} \times 100\%,\ \delta'_H = \frac{\Delta S_{mC} + \Delta S_n}{\Delta S} \times 100\% \tag{15}$$

2.3.5. Trend and Change Point Analysis

In this paper, the linear regression method and Mann–Kendall non-parametric statistical test method [42,43] were used to reveal the variation trend in the time series of the runoff, sediment discharge, and influencing factors. The change point analysis was conducted by the Mann–Kendall and Pettitt mutation tests [44,45], supplementarily testified by the change point of the cumulative anomaly curve. The Mann–Kendall method has no requirements for the distribution of sample data and has good applicability to hydrometeorological data with a non-normal distribution [46].

3. Results

3.1. Interannual Variation of Runoff and Sediment Discharge

The runoff in the Taohe River Basin showed a significant downward trend from 1956–2019 at the Hongqi hydrological station, with a linear change rate of -0.28×10^8 m^3/a. The M-K statistic was −2.61, reaching the significance level of 0.05. The annual average runoff was 44.90×10^8 m^3. The average runoff from 1956–1986 was 52.13×10^8 m^3, higher than the annual average runoff by 16.10%. The runoff fell by 26.88% during 1987–2019 (38.12×10^8 m^3); this was less than the annual average runoff by 15.10%. The interannual variation in runoff is shown in Figure 2a. The M-K test in Figure 2c, the Pettitt mutation test, and the cumulative anomaly curves show that the annual runoff mutated in 1987 at a 95% confidence level, and showed no significant upward trend from 1956–1987, with UFk > 0 in most years, but it did not reach the significance level of 0.05. It significantly decreased from 1987–2002, with UFk < 0, and reached the significance level of 0.05 in 1998.

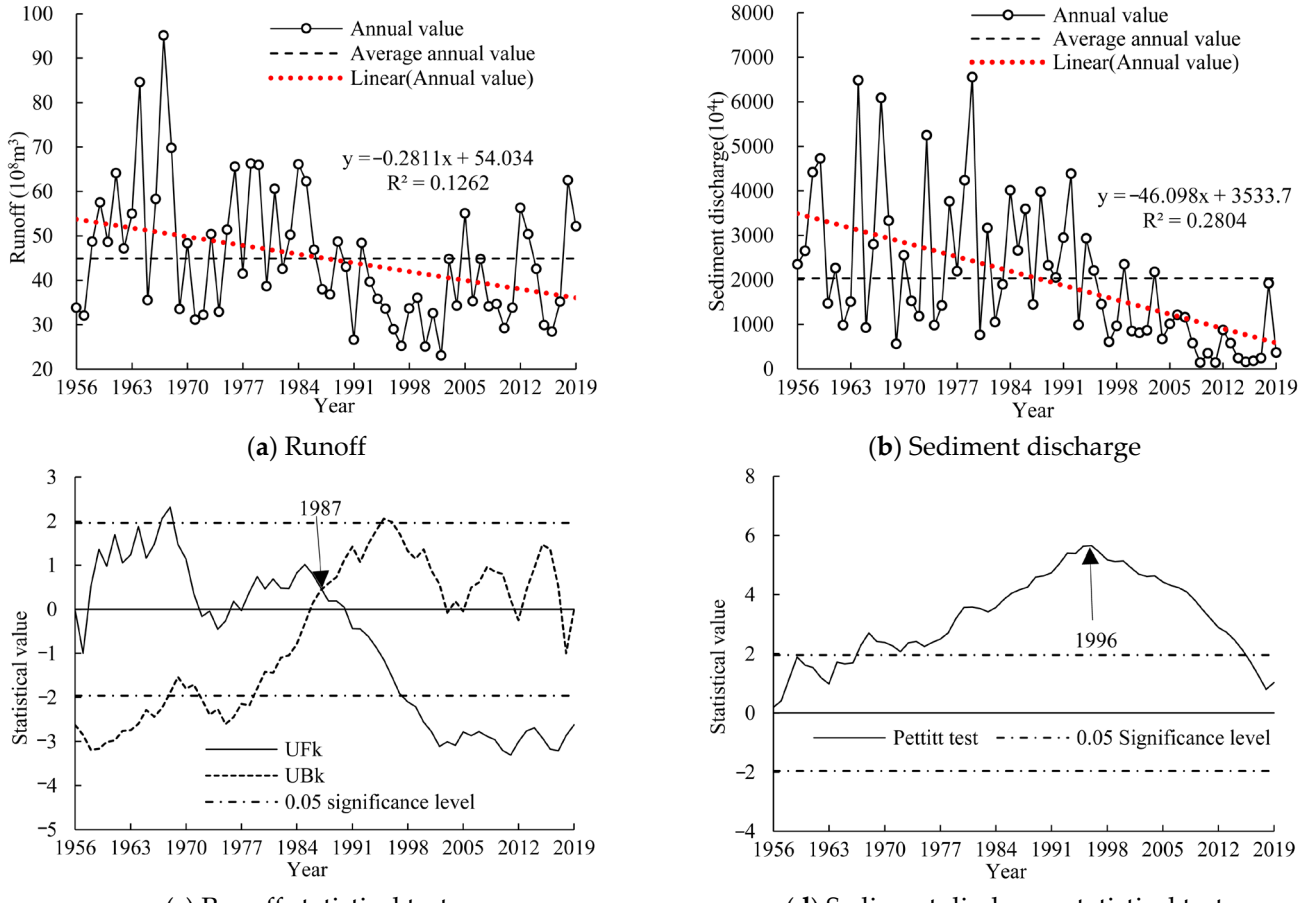

Figure 2. Interannual variation and change points of runoff and sediment discharge in Taohe River Basin. (**a**) Runoff; (**b**) sediment discharge; (**c**) runoff statistical test; (**d**) sediment discharge statistical test.

The sediment discharge in the Taohe River Basin showed a significant downward trend from 1956–2019 at the Hongqi hydrological station, with a linear change rate of -46.10×10^4 t/a. The M-K statistic was −5.03, reaching a significance level of 0.05. The annual average sediment discharge was 2035.57×10^4 t. Compared with the average sediment discharge from 1956–1995, the sediment discharge fell by 70.12% from 1996–2019. It was 2761.78×10^4 t from 1956–1995, higher than the annual average sediment discharge by 35.68%, and it was 825.22×10^4 t from 1996–2019, lower than the annual average sediment discharge by 59.46%. The interannual variation of sediment discharge is shown

in Figure 2b. Both the Pettitt mutation test in Figure 2d and the cumulative anomaly curve showed that the annual sediment discharge displayed a sudden change in 1996, increasing from 1956 to 1995 and decreasing from 1996 to 2019.

3.2. Spatiotemporal Variation of Driving Variables

3.2.1. Temporal and Spatial Variations of Rainfall and Rainfall Erosivity

Based on the rainfall data of 19 meteorological stations in the Taohe River Basin from 1960–2019, the annual rainfall (P) and annual rainfall erosivity (R) of the stations were calculated to obtain the annual P and R of the basin using the Thiessen polygon weighted method. P and R displayed no obvious change trends, and M-K statistics did not reach the significance level of 0.05 (Figure 3). The annual average values of P and R were 553.14 mm and 880.57 MJ·mm·(hm^2·h·a)$^{-1}$, respectively. The M-K mutation test showed that P and R did not display mutations, and fluctuated within a certain range of the annual average value.

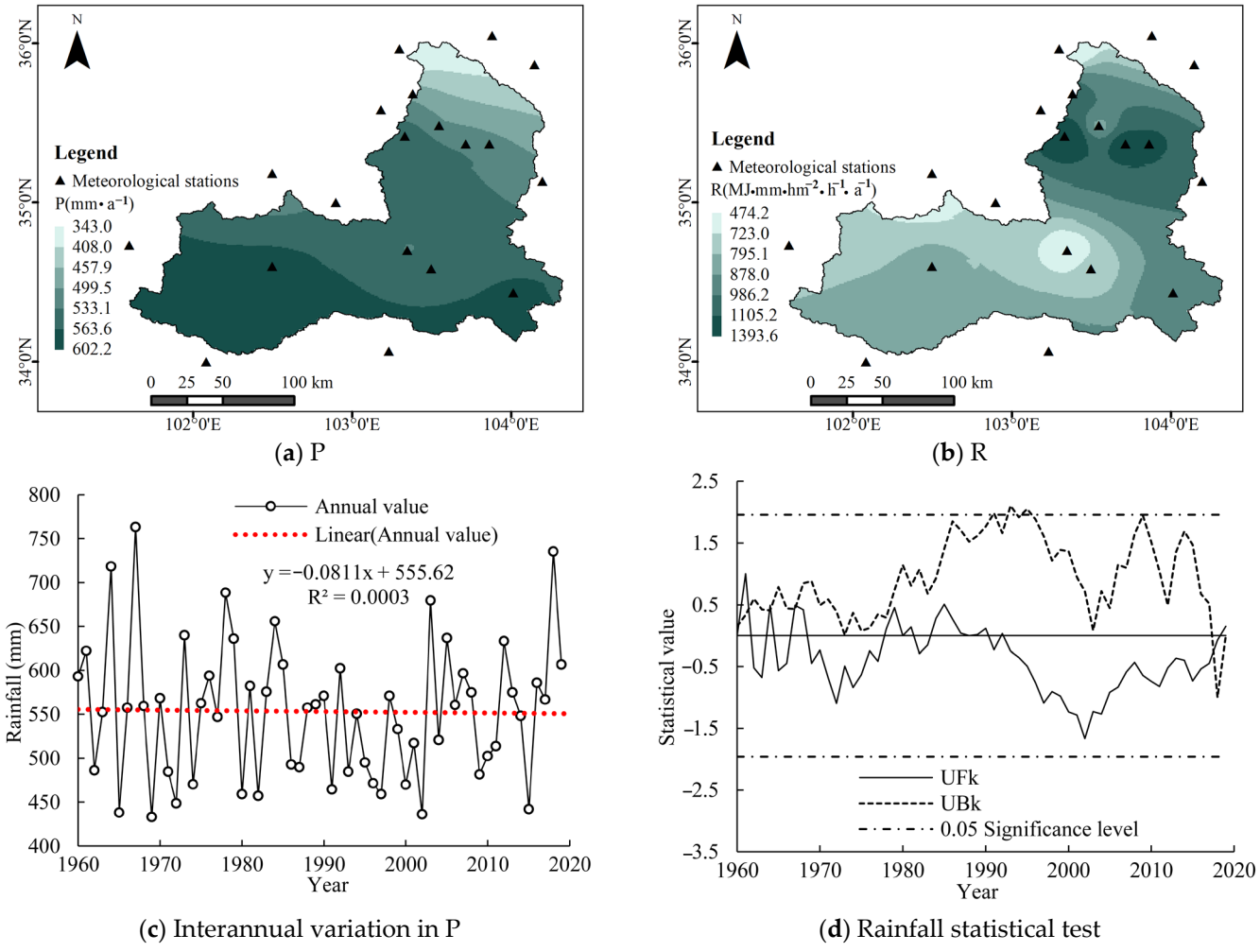

Figure 3. Spatial distribution of annual average rainfall and rainfall erosivity in Taohe River Basin (**a**) P; (**b**) R; (**c**) Interannual variation in P; (**d**) Rainfall statistical test.

The spatial distribution of rainfall P and rainfall erosivity R in the Taohe River Basin were obtained using inverse distance weighted interpolation. The spatial distributions of the annual averages of P and R are shown in Figure 3. P decreases gradually from south to north. The rainfall in the upper reaches of the basin is the highest, and it is distributed in eastern Henan Mongolian Autonomous County and Luqu County, with an annual rainfall of 563.60~602.23 mm. The rainfall in the middle reaches is between 533.09 and 563.60 mm;

the middle reaches are located in the southern part of Xiahe County, Zhuoni County, Lintan County, and the northern part of Minxian County. The rainfall in the lower reaches is the lowest, with annual rainfall between 342.97 and 533.09 mm. An obvious difference in spatial distribution exists between R and P. R in the middle reaches is the lowest, and it is larger in the upstream and downstream regions. The lower-value area is located in southern Xiahe County, central Zhuoni County, and southwestern Lintan County in the upper and middle reaches, with R between 474.18 and 878.01 $MJ \cdot mm \cdot (hm^2 \cdot h \cdot a)^{-1}$. The larger-value area is located in Kangle County, eastern Dongxiang Autonomous County, Hezheng County, Guanghe County, southern Lintao County, and western Weiyuan County, with R between 986.18 and 1393.62 $MJ \cdot mm \cdot (hm^2 \cdot h \cdot a)^{-1}$.

In conclusion, the spatial distribution of P and R is inconsistent. P gradually decreases from the upper reaches to the lower reaches, while R presents a small value in the upper and middle reaches, and a large value in the lower reaches. The rainfall erosivity in the lower reaches with a small amount of rainfall is larger, while the rainfall erosivity in the upper and middle reaches with a relatively large amount of rainfall is smaller. Although the amount of rainfall in the lower reaches of the Taohe River Basin is small, the rainfall intensity is large and concentrated, and the degree of non-uniformity is high, resulting in large erosive rainfall. Meanwhile, there are many loess hills in the lower reaches with fragmented terrain and poor vegetation coverage, resulting in serious soil and water loss in the lower reaches. The middle and upper reaches of the river have large rainfall, but the rainfall intensity is small and non-concentrated, while the erosive rainfall is small, and the erosive power of the rainfall is relatively weak. Meanwhile, the upper and middle reaches of the river are plateau and alpine canyon areas with good vegetation conditions, and the sediment yield is relatively small and the runoff is large. Water and sand in the Taohe River Basin have different sources, with the middle reaches producing water and the lower reaches producing sand.

3.2.2. Temporal and Spatial Variations in Potential Evapotranspiration

ET_0 showed a significant upward trend in the Taohe River Basin from 1960–2019, with a linear change rate of 0.93 mm/a. The M-K statistic was 4.31, reaching the significance level of 0.05. The annual average ET_0 was 819.46 mm. Compared with the average value from 1960–1995, ET_0 increased by 4.71% from 1996–2019. It was 804.31 mm from 1960–1995, less than the annual average ET_0 by 1.85%, and it was 842.20 mm from 1996–2019, higher than the annual average ET_0 by 2.77%. The M-K mutation analysis showed that, within the 95% confidence interval, ET_0 mutated in 1995 and showed an insignificant upward trend from 1960 to 1995, with UFk > 0 in most years and without reaching the significance level of 0.05. It showed a significant upward trend from 1996 to 2019, with UFk > 0 and reaching the significance level of 0.05 in 2000.

Spatial interpolation of the ET_0 in the Taohe River Basin was carried out based on the inverse distance weighted interpolation method by GIS. The spatial distribution of the annual average ET_0 is shown in Figure 4. ET_0 in the upper reaches is the smallest, followed by that in the middle reaches, and ET_0 in the lower reaches is the largest. ET_0 in the upper reaches is between 779.75 and 821.49 mm, and increases in the middle reaches. The maximum ET_0 is in the lower reaches, ranging between 893.95 and 927.58 mm and increasing from south to north. The spatial variation in ET_0 is related to the geographical environment. ET_0 in the upper and middle reaches is low because of high altitude, low temperature, heavy rainfall, and high relative humidity. ET_0 in the lower reaches is high because of low altitude, high temperature, little rainfall, and low relative humidity.

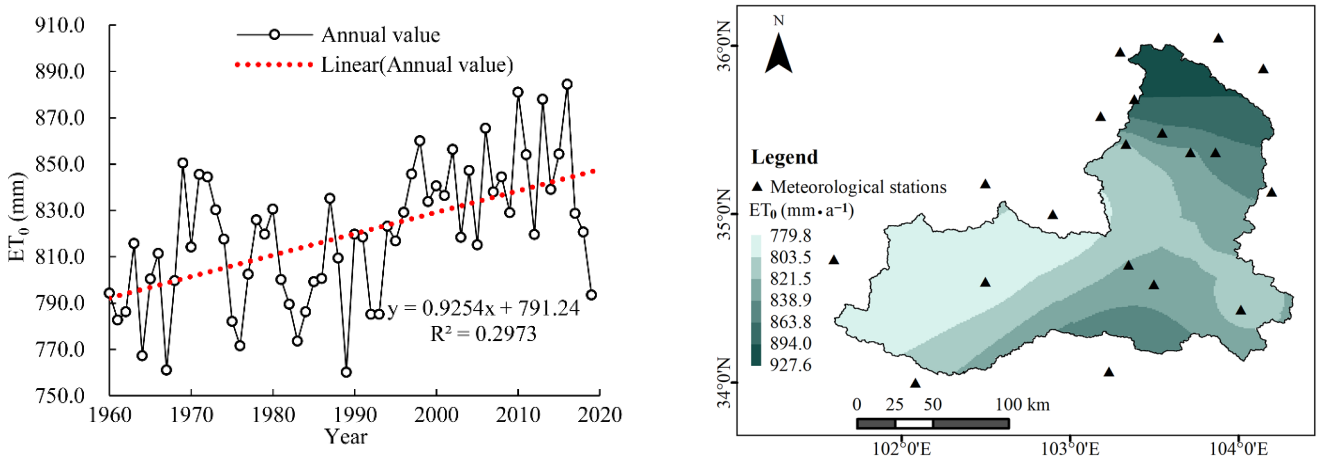

(**a**) Interannual variation of ET_0 (**b**) Spatial distribution of ET_0

Figure 4. Interannual variation and spatial distribution of ET_0 in Taohe River Basin. (**a**) Interannual variation of ET_0; (**b**) Spatial distribution of ET_0.

3.2.3. Interannual Variation of Sediment Concentration

The sediment concentration C showed a significant downward trend in Taohe River Basin from 1960–2019, with a linear change rate of −0.06 kg/m^3 (Figure 5). The M-K statistic was −3.67, reaching a significance level of 0.05. The annual average sediment concentration was 4.05 kg/m^3. Compared with the average value from 1960–2006, sediment concentration fell by 76.06% from 2007–2019. It was 4.85 kg/m^3 from 1960–2006, higher than the annual average sediment concentration by 19.73%. It was 1.16 kg/m^3 from 2007–2019, lower than the annual average sediment concentration by 71.34%. M-K mutation analysis showed that within the 95% confidence interval, sediment concentration mutated in 2007 and showed a non-significant increase from 1960 to 2006, with UFk > 0 in most years and not reaching the significance level of 0.05. It showed a significant decrease from 2007 to 2019, with UFk < 0, and reached the significance level of 0.05 in 2012.

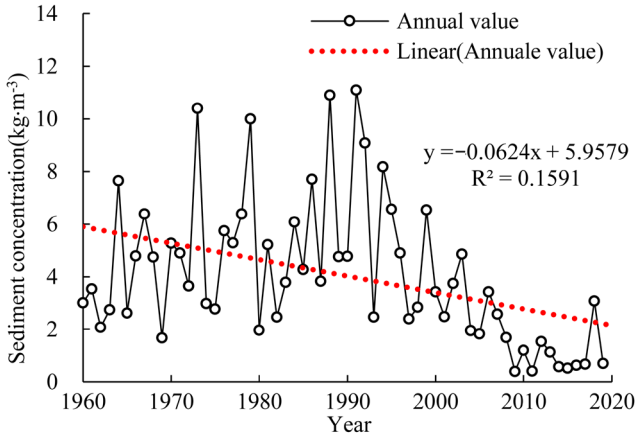

Figure 5. Interannual variation of sediment concentration in Taohe River Basin.

3.3. Qualitative Analysis of Driving Variables

3.3.1. Correlation Coefficient between Runoff and Driving Variables

Based on the Budyko hypothesis and water balance equation, the function relationship of Q = f(P, ET_0, n) was established. The factors affecting the change in runoff included rainfall, potential evapotranspiration, and surface characteristics. Pearson and Kendall correlation coefficients were used to reveal the relationship between the three variables of runoff, rainfall, and potential evapotranspiration. The correlation coefficients between

the three variables are shown in Table 1. The results show that the correlation coefficient between runoff and rainfall Cor_Q-P (0.52~0.70) is larger than that between runoff and potential evapotranspiration Cor_Q-ET_0 (0.30~0.33). Compared with ET_0, runoff is more closely related to rainfall, and runoff change is more affected by rainfall.

Table 1. Correlation coefficient between runoff and related variables.

Correlation Coefficient	P		ET_0	
	Pearson	Kendall	Pearson	Kendall
Q	0.698 **	0.520 **	0.325 **	0.302 **
P			0.752 **	0.584 **

Note: ** 0.01 significance level, Pearson and Kendall respectively represent Pearson correlation coefficient and Kendall correlation coefficient.

3.3.2. Correlation Coefficient between Sediment Discharge and Driving Variables

Based on the Budyko hypothesis and the water–sediment relationships, the function relationship of S = f(P, ET_0, n, C) was established. The factors influencing the change in sediment discharge include rainfall P, potential evapotranspiration ET_0, surface characteristics n, and sediment concentration C. The correlation coefficients between the four variables are shown in Table 2. The order of correlation coefficients is Cor_S-C (0.81~0.86), Cor_S-R (0.69~0.71), Cor_S-P (0.63~0.67), and Cor_S-ET_0 (0.35~0.52). Sediment concentration is the most important factor affecting the change in sediment discharge, and the influence of potential evapotranspiration is the least important factor. Sediment concentration reflects soil and water loss in the basin and is significantly affected by human activities involving conservation measures. The change in sediment concentration is closely related to human activities, and sediment concentration can be regarded as a variable representing the influence of human activities. Considering the variables in the universal soil erosion equation (USLE), the rainfall kinetic energy factor is controlled by the variation in rainfall. Compared with rainfall, the change in sediment discharge has a stronger correlation with rainfall erosivity over time, and erosive rainfall promotes the change in sediment production and sediment discharge. Since the rainfall P and rainfall erosivity R in the Taohe River Basin show an insignificant trend over the years, the influence of rainfall is not obvious. In conclusion, the change in sediment discharge is closely related to human activities, followed by the influence of climate change (e.g., involving rainfall and potential evaporation).

Table 2. Correlation coefficient between sediment discharge and related variables.

Correlation Coefficient	C		P		R		ET_0	
	Pearson	Kendall	Pearson	Kendall	Pearson	Kendall	Pearson	Kendall
S	0.810 **	0.858 **	0.625 **	0.672 **	0.714 **	0.693 **	0.354 **	0.519 **
C			0.629 **	0.646 **	0.650 **	0.666 **	0.507 **	0.560 **
P					0.903 **	0.830 **	0.752 **	0.584 **
R							0.601 **	0.606 **

Note: ** 0.01 significance level; Pearson and Kendall respectively represent Pearson correlation coefficient and Kendall correlation coefficient.

3.3.3. Regression Relationship between Runoff and Driving Variables

According to the long-term time series of annual rainfall, potential evapotranspiration, and runoff in the basin, the regression curves of P-Q and ET_0-Q were constructed, as shown in Figure 6. The results show that runoff is closely related to rainfall, and P-Q (determination coefficient R^2 = 0.63) has a better linear relationship than ET_0-Q (determination coefficient R^2 = 0.42). Rainfall has a greater impact on runoff, and the increase in rainfall leads to an increase in runoff. P-Q showed a good linear relationship between 1960–1986 (R^2 = 0.80) and 1987–2019 (R^2 = 0.67), and the slope decreased from 0.64 (1960–1986) to 0.46 (1987–2019), indicating that the influence of rainfall in the Taohe River Basin became smaller from 1987–2019. The correlation between P and Q was reduced by human activities, and the

influence of human activities on Q was increased. Meanwhile, it was verified in Section 3.1 that the runoff mutated in 1987, and 1987 was used to divide the base period (1960–1986) and the change period (1987–2019). The change period was greatly influenced by human activities. ET_0 and Q showed reverse changes, with potential evaporation increasing and runoff decreasing. After 1987, the absolute values of R^2 and the slope of the ET_0-Q regression equation decreased, indicating that the effects of climate change, such as ET_0, were weakened, and the effects of human activities increased during the change period. In conclusion, runoff was more closely related to rainfall, and rainfall had a greater impact on runoff. Compared with the base period, the impact of climate change decreased and the impact of human activities increased in the change period.

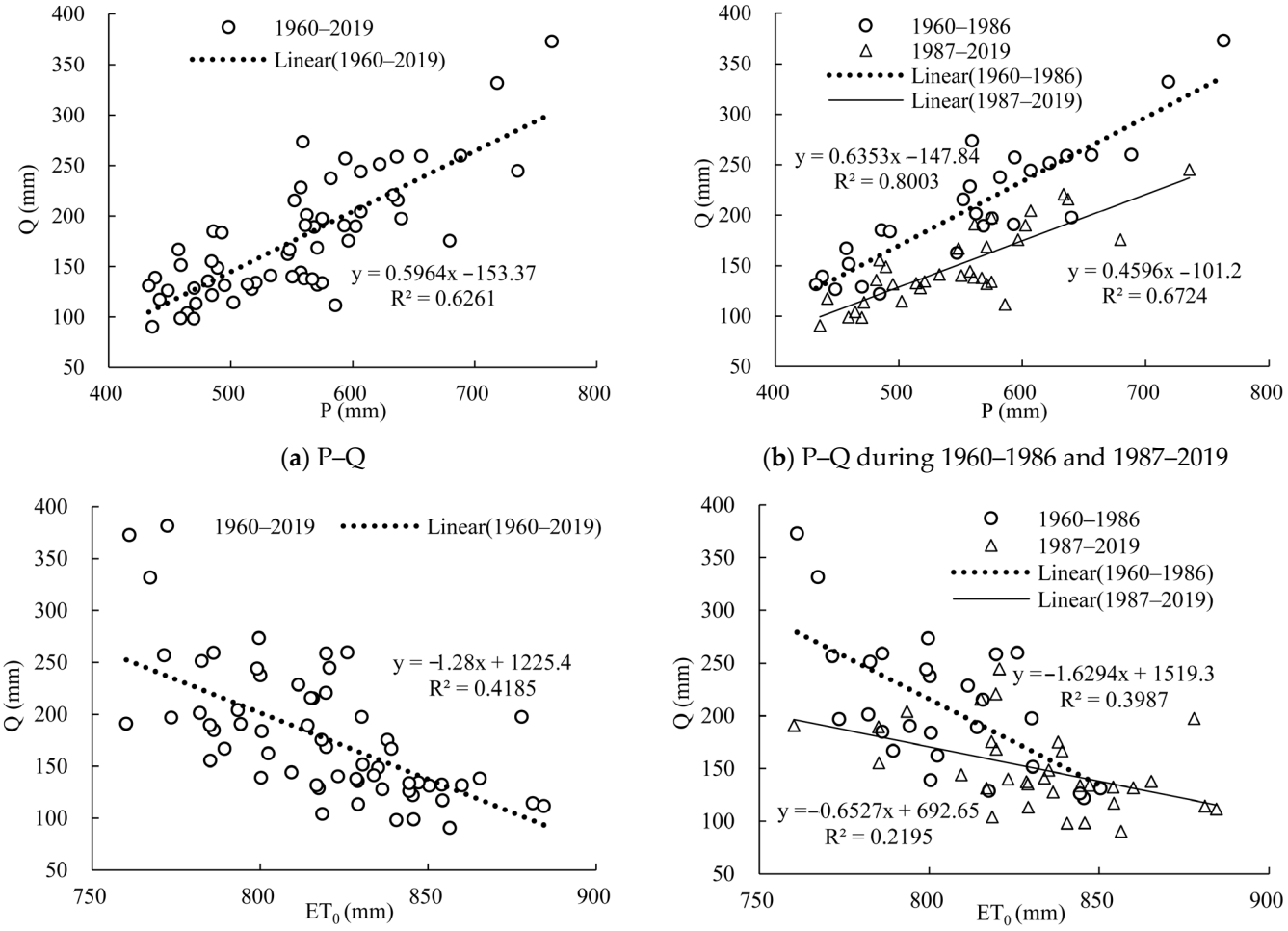

Figure 6. Regression relationship between runoff and related variables in Taohe River Basin. (**a**) P–Q; (**b**) P–Q during 1960–1986 and 1987–2019; (**c**) ET_0-Q; (**d**) ET_0-Q during 1960–1986 and 1987–2019.

3.3.4. Regression Relationship between Sediment Discharge and Driving Variables

Based on the long-term time series of annual rainfall P, potential evapotranspiration ET_0, annual average sediment concentration C, runoff Q, and sediment discharge S, the regression curves of Q–S, P–S, ET_0–S, and C–S were constructed, as shown in Figure 7. The determination coefficient R^2 shows that the order of influencing the change in sediment discharge is sediment concentration (0.73), runoff (0.50), rainfall (0.33), and potential evapotranspiration (0.28). Sediment concentration mainly represents the influence of human activities. Therefore, the change in sediment discharge is most closely related to the influence of human activities, followed by climatic factors such as rainfall and potential evapotranspiration. It was verified in Section 3.1 that the sediment discharge mutated

in 1996, and 1996 was used to divide the base period (1960–1995) and the change period (1996–2019). The regression curve of P–S from 1960 to 1995 (R^2 = 0.65) showed a better linear relationship than that from 1996 to 2019 (R^2 = 0.18), with the slope decreasing from 6.39 to 1.38. The correlation between P and S was weakened, and the change rate (slope) in sediment yield by precipitation decreased from 1996–2019, when the sediment discharge change caused by changes in unit precipitation became smaller and the impact of human activities increased. C–S showed a good linear relationship between 1960–1995 (R^2 = 0.61) and 1996–2019 (R^2 = 0.81). The sediment concentration and sediment discharge were closely related. The slope decreased from 188.28 to 135.94 mm, and the change rate in sediment discharge by sediment concentration decreased, indicating that the influence of human activities increased and the impact of climate change was reduced during 1996–2019. In conclusion, the relationship between sediment concentration and sediment discharge was the most significant. Compared with the base period (1960–1995), the influence of human activities increased and the influence of climate change decreased during the change period (1996–2019).

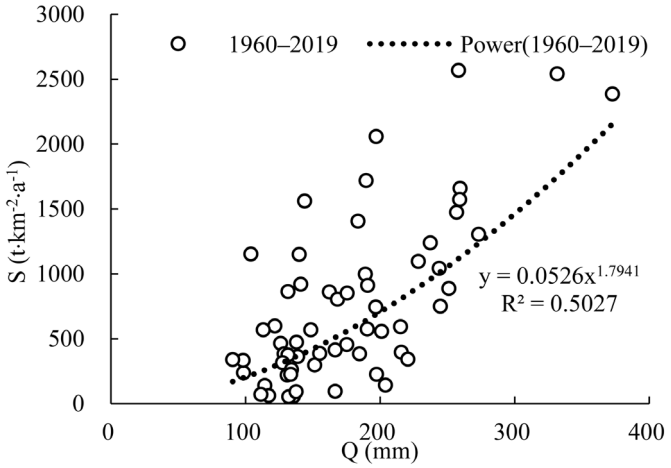

(**a**) Q–S

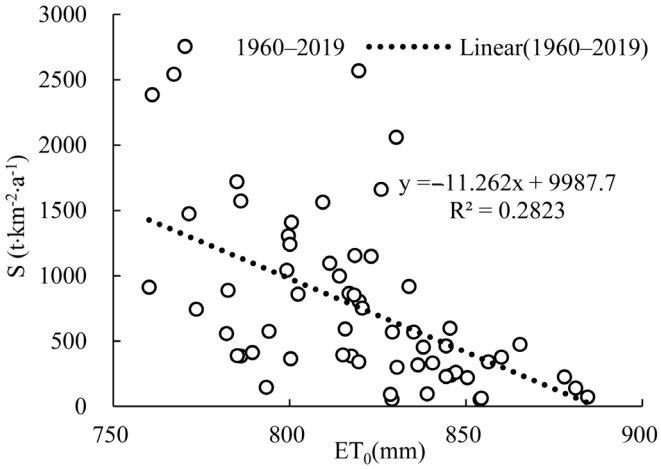

(**b**) ET₀–S

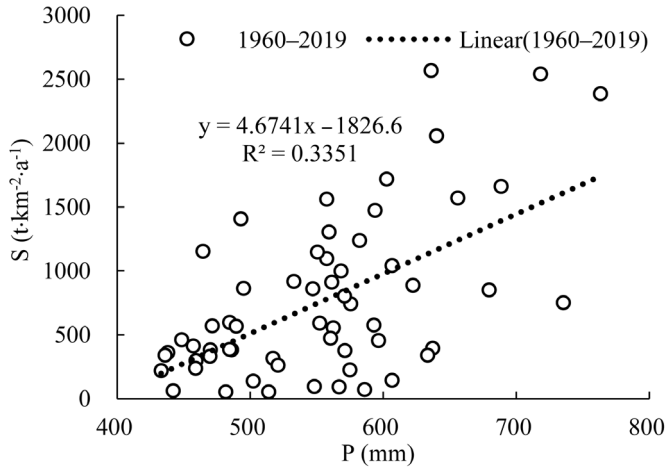

(**c**) P–S

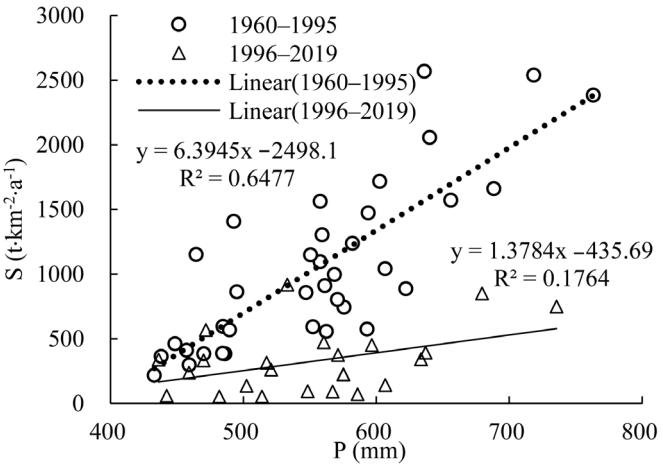

(**d**) P–S during 1960–1995 and 1996–2019

Figure 7. *Cont.*

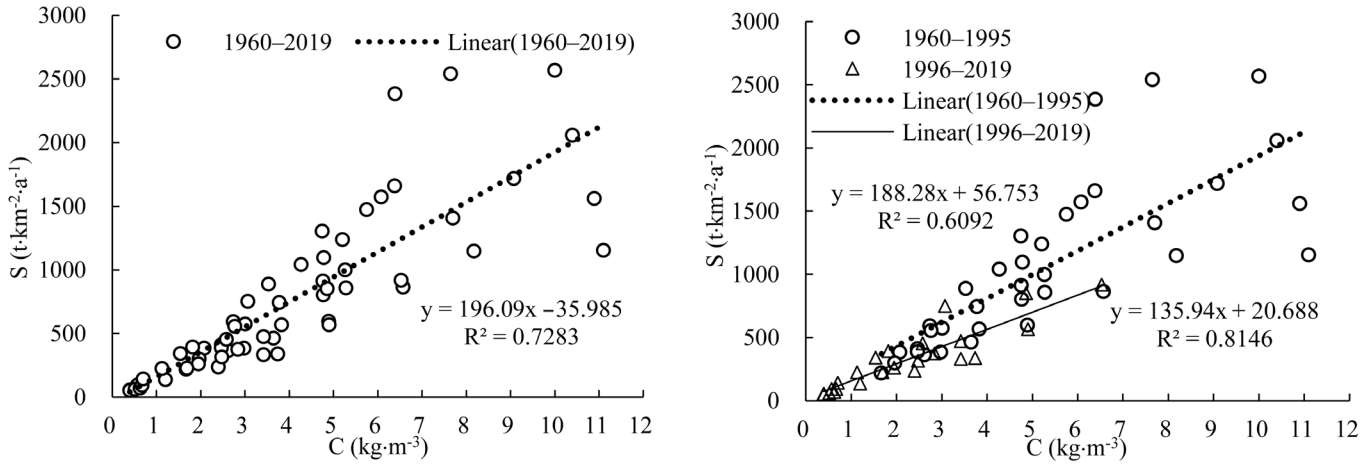

(**e**) C–S (**f**) C–S during 1960–1995 and 1996–2019

Figure 7. Regression relationship between sediment discharge and related variables in Taohe River Basin. (**a**) Q–S; (**b**) ET_0–S; (**c**) P–S; (**d**) P–S during 1960–1995 and 1996–2019; (**e**) C–S; (**f**) C–S during 1960–1995 and 1996–2019.

3.4. Quantitative Analysis of driving Variables

3.4.1. Quantitative Analysis of the Attribution of Runoff Change

Based on the analysis results of the long time series of annual runoff in Section 3.1, and taking 1987 as the mutation point, it was divided into a base period (1960–1986) and a change period (1987–2019). The change period (1987–2019) was divided into four periods: 1987–1989, 1990–1999, 2000–2009, 2010–2019, which could represent different generations. Compared with the base period, the runoff depth in the change period showed a statistically significant decrease, with a decrease of 60.22 mm. The changes in runoff influenced by P, ET_0, and surface characteristics n were 9.87 mm, 4.78 mm, and 45.57 mm, respectively, and the contribution rates were 16.40%, 7.94%, and 75.67%, respectively. It can be concluded that the contribution rate of climate change was 24.33%, and that of human activities was 75.67%. Human activities were the main factor affecting runoff change. In the 1990s, 2000s, and 2010s, the results showed that the contribution rates of climate change were 36.60%, 21.64%, and 5.53%, respectively. The contribution rate of climate change gradually decreased, and that of human activities increased continuously, namely by 63.40%, 78.36%, and 94.47%, respectively. The elasticity coefficient ε_P is positive, indicating that P changed in the same direction as Q, and the elasticity coefficient ε_{ET0} is negative, indicating that ET_0 changed in the opposite direction of Q. The results are shown in Table 3.

Table 3. Contribution of influencing factors to runoff change.

Period	Q/mm	P/mm	ET_0/mm	ε_P	ε_{ET0}	ε_n	ΔQ/mm	ΔP/mm	ΔET_0/mm	Δn/mm	δp/%	δ_{ET0}/%	δn/%
1960–1986	209.62	562.72	803.77	1.59	−0.70	−0.97	.						
1987–2019	149.40	545.31	832.30	2.07	−0.93	−1.33	60.22	9.87	4.78	45.57	16.40	7.94	75.67
1987–1989	161.23	536.11	801.58	1.91	−0.86	−1.21	48.39	15.29	−0.38	33.48	31.59	−0.78	69.19
1990–1999	137.42	520.26	821.73	2.10	−0.95	−1.39	72.20	23.56	2.87	45.78	32.63	3.97	63.40
2000–2009	142.51	547.44	839.06	2.17	−0.98	−1.40	67.11	8.64	5.88	52.59	12.88	8.76	78.36
2010–2019	164.72	570.99	845.33	2.00	−0.90	−1.26	44.90	−4.79	7.27	42.42	−10.66	16.19	94.47

Note: ΔQ, ΔP, ΔET_0, Δn respectively represent the variations of runoff, rainfall, potential evapotranspiration, and underlying surface characteristics, and δ_P, δET_0, δ_n respectively represent rainfall, potential evapotranspiration, and underlying surface contribution rate.

3.4.2. Quantitative Analysis of the Attribution of Sediment Discharge Changes

Based on the analysis results of the long time series of sediment discharge in Section 3.1, and taking 1996 as the mutation point, it was divided into the base period (1960–1995) and the change period (1996–2019). The change period (1996–2019) was divided into three periods: 1996–1999, 2000–2009, 2010–2019, which could represent different generations. Compared with the base period, the sediment delivery modulus decreased significantly in the change period, with a decrease of 725.54 t/km^2. The change in sediment discharge affected by P, ET_0, surface characteristics n, and sediment concentration were 5.11 t/km^2, 13.95 t/km^2, 151.79 t/km^2, and 554.68 t/km^2, respectively, and the contribution rates were 0.70%, 1.92%, 20.92%, and 76.45%, respectively. This indicated that the contribution rate of climate change was 2.63% and that of human activities was 97.37%. Human activities were the main factor affecting the change in sediment discharge. In the 1990s, 2000s, and 2010s, the results showed that the contribution rates of climate change were 24.83%, 3.87%, and −0.32%, respectively, and those of human activities were 75.17%, 96.13%, and 100.32%, respectively. The contribution rate of climate change decreased, and that of human activities increased gradually. Elasticity coefficients η_{mc} and η_P were positive, indicating that sediment concentration, rainfall, and sediment discharge changed in the same direction, while η_{ET0} was negative, indicating that ET_0 and sediment discharge changed in reverse. The decrease in rainfall, sediment concentration, and runoff, or the increase in potential evaporation, made sediment discharge decrease correspondingly, in line with the general law of nature. The results are shown in Table 4.

Table 4. Contributions of influencing factors to sediment discharge change.

Period	S /t/km^2	C /kg/m^3	P /mm	ET_0 /mm	η_{mc}	η_P	η_{ET0}	η_n	ΔS /t/km^2	ΔP /mm	ΔET_0 /mm	Δn /mm	Δmc /kg/m^3	δ'_P /%	δ'_{ET0} /%	δ'_n /%	δ'_{mc} /%
1960–1995	1049.03	5.27	554.72	804.31	0.96	1.68	−0.72	−1.04									
1996–2019	323.49	2.23	550.78	842.20	1.26	2.21	−0.96	−1.43	725.54	5.11	13.95	151.79	554.68	0.70	1.92	20.92	76.45
1996–1999	524.59	4.17	508.63	842.19	1.26	2.25	−0.99	−1.54	524.44	106.82	23.37	219.81	174.43	20.37	4.46	41.91	33.26
2000–2009	369.90	2.64	547.44	839.06	1.29	2.28	−0.99	−1.47	679.13	11.19	15.10	176.03	476.81	1.65	2.22	25.92	70.21
2010–2019	196.64	1.04	570.99	845.33	1.02	1.79	−0.77	−1.13	852.39	−10.06	7.36	40.19	814.90	−1.18	0.86	4.71	95.60

Note: ΔS, ΔP, ΔET_0, Δn, Δmc respectively represent sediment discharge, rainfall, potential evapotranspiration, underlying surface characteristics, and influence variation of sediment concentration, while δ'_P, $\delta'ET_0$, δ'_n, δ'_{mc} respectively represent rainfall, potential evapotranspiration, underlying surface, and contribution rate of sediment concentration.

4. Discussion

The runoff in the Taohe River Basin showed a significant downward trend during 1956–2019, with a linear change rate of -0.28×10^8 m^3/a and a change point in 1987. This is consistent with the conclusion of Cheng L. et al. [47] that "runoff in the upper Taohe River from 1956 to 2014 showed a significant decline of -2.7×10^8 m^3/10a, with the break point occurring in 1987". The changes in the runoff in the period 1956–2019 related to both the natural variability of climate and anthropogenic climate change. Human activities (including soil and water conservation measures, land use changes, and hydraulic engineering construction) change surface conditions and have an impact on hydrological processes, including evapotranspiration and rainfall, leading to climate change, including both the natural variability of climate and anthropogenic climate change. According to the land use situation in the three periods from the 1980s to the 2000s, the farmland first decreased and then increased and then decreased, and the change trend of forest land and grassland was the opposite, which is consistent with the process of deforestation to increased farmland to the implementation of measures for returning farmland to forest and grassland in the Taohe River Basin. The watershed area decreased in the 1980s and increased in the 2000s, and settlement increased, which is consistent with the development of urbanization and the construction of water conservancy projects. Since the 1990s, deforestation and grassland reclamation have seriously damaged vegetation and reduced water-holding capacity, causing serious soil erosion. The construction of two major irrigation districts, the Puji Canal Irrigation District and the Taohui Canal Irrigation District, was completed in the late

1980s, and large-scale water diversion and transfer also occurred in this period, which is consistent with the variations in runoff.

Many methods can be used to quantify the effects of climate change and human activities on runoff, including trend analysis, linear regression models, artificial neural network methods, hydrological models, and Budyko-based methods [48]. The Budyko-based method is relatively simple and reliable compared to other methods, and can be applied with easily available and smaller amounts of data, which have been proven in many studies [49,50]. Based on the Budyko hypothesis theory, $Q = f(P, ET_0, n)$, runoff is a function of rainfall P, potential evapotranspiration ET_0, and watershed catchment characteristics n, while $S = f(P, ET_0, n, C)$, and sediment discharge is a function of rainfall P, potential evapotranspiration ET_0, catchment characteristics n and sediment concentration C, so we have analyzed climate change factors, including P(annual rainfall erosivity R) and ET_0, and human factors, including catchment characteristics n and sediment concentration C. In the process of constructing the model $S = f(P, ET_0, n, C)$, the water–sediment relationship was introduced in $Q = f(P, ET_0, n)$ on the basis of Budyko hypothesis theory, so as to establish a quantitative attribution analysis model for the change in sediment discharge and determine the contribution of climate change and human activities to sediment discharge change. The sensitivity coefficients of runoff and sediment discharge to changes in climatic change and human activities were estimated for the long-term average annual values at the catchment scale [35]. The interannual and intra-annual variability and spatial differences in rainfall P, potential evapotranspiration ET_0, catchment characteristics n, and sediment concentration C were not considered, but it is generally accepted that catchment characteristics vary both spatially and temporally and have an impact on runoff and sediment discharge in the basin [10]. Therefore, the errors from both the Budyko-based model structure and the model parameter n, which we assume to be consistent in time, caused the result that the Budyko-based analysis cannot be free of errors [51,52].

This study not only extends the application of Budyko-based methods, but also combines traditional statistical qualitative analysis with quantitative calculations to distinguish the effects of climate change and human activities on changes in runoff and sediment discharge. The results of the study can be used as a scientific basis to guide local erosion control and the sustainable use of water resources in the basin. In particular, the introduction of the water– sediment relationship into Budyko-based methods and its application to the attribution analysis of sediment discharge are of great significance to extend the Budyko theory.

5. Conclusions

In this study, the linear regression method, Mann–Kendall nonparametric statistical test, Pettitt mutation test, cumulative anomaly curve, and spatial interpolation method were used to analyze the spatiotemporal evolution of runoff and sediment discharge and their driving variables. An analytical method combining traditional qualitative analysis with a quantitative calculation based on Budyko theory and water–sediment relationships was built. The qualitative and quantitative relationships between runoff and sediment discharge changes and their driving variables were discussed to clarify the response mechanism of runoff and sediment discharge changes in the Taohe River Basin. The main conclusions are as follows:

The runoff and sediment discharge in the Taohe River Basin showed a significant downward trend from 1956–2019 and mutated in 1987 and 1996, respectively. Water and sand in the Taohe River Basin have different sources, with the middle reaches producing water and the lower reaches producing sand.

The results of correlation coefficients show that runoff is more closely related to rainfall than ET_0, and the changes in sediment discharge are closely related to human activities, followed by the influence of climate change, such as rainfall and potential evaporation.

The contributions of climate change to the variations in runoff and sediment discharge were 24.33% and 2.63%, respectively, while the contributions of human activities were

75.67% and 97.37%, respectively. Human activities were the main factors influencing the variation in runoff and sediment discharge.

Author Contributions: Data curation, Y.M. and D.S.; formal analysis, Y.M.; funding acquisition, Z.N. and D.S.; supervision, Y.M., Z.N., D.S. and X.W.; writing—original draft preparation, Y.M.; writing—review and editing, Z.N., X.W. and D.S. All authors have read and agreed to the published version of the manuscript.

Funding: This research was funded by the National Natural Science Foundation of China (NSFC) (Grant No.42261003); the Innovation Fund of Higher Education of Gansu Province (Grant No.2021B-120); the Special Project for the Construction of Scientific Research Team of the College of Water Conservancy and Hydropower Engineering, Gansu Agricultural University, China (Grant No. Gaucwky-04); the Key R&D Project of Gansu Province (Grant No.21YF5NA015); the project of the Youth Doctor Foundation for Higher Education in Gansu Province (Grant No.2022QB-070); the Science and Technology Innovation Fund of Gansu Agricultural University—Young Mentor Support Fund Project (Grant No.GAU-QDFC-2021-16).

Data Availability Statement: Data are contained within the article.

Acknowledgments: The authors would like to thank all funders and lab facilities. We also gratefully acknowledge the anonymous reviewers for their constructive comments.

Conflicts of Interest: The authors declare no conflict of interest.

References

1. Feng, X.; Cheng, W.; Fu, B.; Lü, Y. The role of climatic and anthropogenic stresses on long-term runoff reduction from the Loess Plateau, China. *Sci. Total Environ.* **2016**, *571*, 688–698. [CrossRef] [PubMed]
2. Liu, F.; Yang, Q.; Chen, S.; Luo, Z.; Yuan, F.; Wang, R. Temporal and spatial variability of sediment flux into the sea from the three largest rivers in China. *J. Asian Earth Sci.* **2014**, *87*, 102–115. [CrossRef]
3. Wang, S.; Fu, B.; Piao, S.; Lü, Y.; Ciais, P.; Feng, X.; Wang, Y. Reduced sediment transport in the Yellow River due to anthropogenic changes. *Nat. Geosci.* **2016**, *9*, 38–41. [CrossRef]
4. Xu, K.; Milliman, J.D.; Xu, H. Temporal trend of precipitation and runoff in major Chinese Rivers since 1951. *Glob. Planet. Change* **2010**, *73*, 219–232. [CrossRef]
5. Wang, S.; Fu, B.; Liang, W. Developing policy for the Yellow River sediment sustainable control. *Natl. Sci. Rev.* **2016**, *3*, 162–164. [CrossRef]
6. Wang, S.; Fu, B.; Liang, W.; Liu, Y.; Wang, Y. Driving forces of changes in the water and sediment relationship in the Yellow River. *Sci. Total Environ.* **2017**, *576*, 453–461. [CrossRef]
7. Xu, J.; Jiang, X.; Sun, H.; Xu, H.; Zhong, X.; Liu, B.; Li, L. Driving forces of nature and human activities on water and sediment changes in the middle reaches of the Yellow River in the past 100 years. *J. Soil Sediment* **2021**, *21*, 2450–2464. [CrossRef]
8. Chu, H.; Wei, J.; Qiu, J.; Li, Q.; Wang, G. Identification of the impact of climate change and human activities on rainfall-runoff relationship variation in the Three-River Headwaters region. *Ecol. Indic.* **2019**, *106*, 105516. [CrossRef]
9. Huntington, T.G. Evidence for intensification of the global water cycle: Review and synthesis. *J. Hydrol.* **2006**, *319*, 83–95. [CrossRef]
10. Chang, J.; Zhang, H.; Wang, Y.; Zhu, Y. Assessing the impact of climate variability and human activities on streamflow variation. *Hydrol. Earth Syst. Sci.* **2016**, *20*, 1547–1560. [CrossRef]
11. Zhao, G.; Tian, P.; Mu, X.; Jiao, J.; Wang, F.; Gao, P. Quantifying the impact of climate variability and human activities on streamflow in the middle reaches of the Yellow River basin, China. *J. Hydrol.* **2014**, *519*, 387–398. [CrossRef]
12. Zhao, Y.; Zou, X.; Gao, J.; Xu, X.; Wang, C.; Tang, D.; Wang, T.; Wu, X. Quantifying the anthropogenic and climatic contributions to changes in water discharge and sediment load into the sea: A case study of the Yangtze River, China. *Sci. Total Environ.* **2015**, *536*, 803–812. [CrossRef]
13. Chen, T.; Ao, T.; Zhang, X.; Li, X.; Yang, K. Climate Change Characteristics of Extreme Temperature in the Minjiang River Basin. *Adv. Meteorol.* **2019**, *2019*, 1935719. [CrossRef]
14. Zhao, G.; Gao, P.; Tian, P.; Sun, W.; Hu, J.; Mu, X. Assessing sediment connectivity and soil erosion by water in a representative catchment on the Loess Plateau, China. *Catena* **2020**, *185*, 104284. [CrossRef]
15. Kong, D.; Miao, C.; Wu, J.; Duan, Q. Impact assessment of climate change and human activities on net runoff in the Yellow River Basin from 1951 to 2012. *Ecol. Eng.* **2016**, *91*, 566–573. [CrossRef]
16. Wu, L.; Wang, S.; Bai, X.; Luo, W.; Tian, Y.; Zeng, C.; Luo, G.; He, S. Quantitative assessment of the impacts of climate change and human activities on runoff change in a typical karst watershed, SW China. *Sci. Total Environ.* **2017**, *601–602*, 1449–1465. [CrossRef] [PubMed]
17. Jia, L.; Yu, K.; Li, Z.; Li, P.; Zhang, J.; Wang, A.; Ma, L.; Xu, G.; Zhang, X. Temporal and spatial variation of rainfall erosivity in the Loess Plateau of China and its impact on sediment load. *Catena* **2022**, *210*, 105931. [CrossRef]

18. Dang, S.; Liu, X.; Yin, H.; Guo, X. Prediction of sediment yield in the middle reaches of the Yellow River Basin under extreme precipitation. *Front. Earth Sci.* **2020**, *8*, 542686. [CrossRef]
19. Li, T.; Wang, S.; Liu, Y.; Fu, B.; Zhao, W. Driving forces and their contribution to the recent decrease in sediment flux to ocean of major rivers in China. *Sci. Total Environ.* **2018**, *634*, 534–541. [CrossRef]
20. Soksamnang, K.; He, H.M.; Zhao, H.F.; Jing, Z.W. Analysis of rainfall erosivity change and its impacts on soil erosion on the Loess Plateau over more than 50 years. *Res. Soil Water Conserv.* **2018**, *25*, 1–7. (In Chinese)
21. Wu, J.; Miao, C.; Wang, Y.; Duan, Q.; Zhang, X. Contribution analysis of the long-term changes in seasonal runoff on the Loess Plateau, China, using eight Budyko-based methods. *J. Hydrol.* **2017**, *545*, 263–275. [CrossRef]
22. Yang, L.; Zhao, G.; Tian, P.; Mu, X.; Tian, X.; Feng, J.; Bai, Y. Runoff changes in the major river basins of China and their responses to potential driving forces. *J. Hydrol.* **2022**, *607*, 127536. [CrossRef]
23. Xu, R.; Qiu, D.; Wu, C.; Mu, X.; Zhao, G.; Sun, W.; Gao, P. Quantifying climate and anthropogenic impacts on runoff using the SWAT model, a Budyko-based approach and empirical methods. *Hydrol. Sci. J.* **2023**, *68*, 1–14. [CrossRef]
24. Song, X.; Sun, W.; Zhang, Y.; Song, S.; Li, J.; Gao, Y. Using hydrological modelling and data-driven approaches to quantify mining activities impacts on centennial streamflow. *J. Hydrol.* **2020**, *585*, 124764. [CrossRef]
25. Hu, Y.; Duan, W.; Chen, Y.; Zou, S.; Kayumba, P.M.; Sahu, N. An integrated assessment of runoff dynamics in the Amu Darya River Basin: Confronting climate change and multiple human activities, 1960–2017. *J. Hydrol.* **2021**, *603*, 126905. [CrossRef]
26. Li, C.; Hao, J.; Zhang, G.; Fang, H.; Wang, Y.; Lu, H. Runoff variations affected by climate change and human activities in Yarlung Zangbo River, southeastern Tibetan Plateau. *Catena* **2023**, *230*, 107184. [CrossRef]
27. Sun, X.; Wang, J.; Ma, M.; Han, X. Attribution of Extreme Drought Events and Associated Physical Drivers across Southwest China Using the Budyko Framework. *Remote Sens.* **2023**, *15*, 2702. [CrossRef]
28. Sun, L.; Wang, Y.; Zhang, J.; Yang, Q.; Bao, Z.; Guan, X.; Guan, T.; Chen, X.; Wang, G. Impact of environmental change on runoff in a transitional basin: Tao River Basin from the Tibetan Plateau to the Loess Plateau, China. *Adv. Clim. Change Res.* **2019**, *10*, 214–224. [CrossRef]
29. Yang, L.; Feng, Q.; Li, C.; Si, J.; Wen, X.; Yin, Z. Detecting climate variability impacts on reference and actual evapotranspiration in the Taohe River Basin, NW China. *Hydrol. Res.* **2016**, *48*, 596–612. [CrossRef]
30. Zhang, W.B.; Xie, Y.; Liu, B.Y. Rainfall erosivity estimation using daily rainfall amounts. *Sci. Geogr. Sin.* **2002**, *22*, 705–711. (In Chinese)
31. Allen, R.G.; Pereira, L.S.; Raes, D.; Smith, M. *Crop Evapotranspiration-Guidelines for Computing Crop Water Requirements-FAO Irrigation and Drainage Paper 56*; FAO: Rome, Italy, 1998; Volume 300, p. D5109.
32. Wu, L.; Liu, X.; Ma, X. Spatiotemporal distribution of rainfall erosivity in the Yanhe River watershed of hilly and gully region, Chinese Loess Plateau. *Environ. Earth Sci.* **2016**, *75*, 315. [CrossRef]
33. Wang, Z.; Xie, P.; Lai, C.; Chen, X.; Wu, X.; Zeng, Z.; Li, J. Spatiotemporal variability of reference evapotranspiration and contributing climatic factors in China during 1961–2013. *J. Hydrol.* **2017**, *544*, 97–108. [CrossRef]
34. Yin, Y.; Wu, S.; Chen, G.; Dai, E. Attribution analyses of potential evapotranspiration changes in China since the 1960s. *Theor. Appl. Climatol.* **2010**, *101*, 19–28. [CrossRef]
35. Sposito, G. Understanding the Budyko Equation. *Water* **2017**, *9*, 236. [CrossRef]
36. Budyko, M.I. *Climate and Life*; Academic Press: New York, NY, USA, 1974.
37. Hankey, A.; Stanley, H.E. An alternate formulation of the static scaling hypothesis. *Int. J. Quantum. Chem.* **1971**, *5*, 593–604. [CrossRef]
38. Choudhury, B. Evaluation of an empirical equation for annual evaporation using field observations and results from a biophysical model. *J. Hydrol.* **1999**, *216*, 99–110. [CrossRef]
39. Yang, H.; Yang, D.; Lei, Z.; Sun, F. New analytical derivation of the mean annual water-energy balance equation. *Water Resour. Res.* **2008**, *44*, W3410. [CrossRef]
40. Schaake, J.C. From climate to flow. In *Climate Change and US Water Resources*; John Wiley: New York, NY, USA, 1990; pp. 177–206.
41. Zheng, H.; Miao, C.; Wu, J.; Lei, X.; Liao, W.; Li, H. Temporal and spatial variations in water discharge and sediment load on the Loess Plateau, China: A high-density study. *Sci. Total Environ.* **2019**, *666*, 875–886. [CrossRef]
42. Kendall, M.G. *Rank Correlation Methods*; Griffin: London, UK, 1948.
43. Mann, H.B. Nonparametric Tests Against Trend. *Econometrica* **1945**, *13*, 245–259. [CrossRef]
44. Hamed, K.H.; Ramachandra Rao, A. A modified Mann-Kendall trend test for autocorrelated data. *J. Hydrol.* **1998**, *204*, 182–196. [CrossRef]
45. Pettitt, A.N. A Non-Parametric Approach to the Change-Point Problem. *Appl. Stat.* **1979**, *28*, 126–135. [CrossRef]
46. Sung, J.H.; Chung, E.; Kim, Y.; Lee, B. Meteorological hazard assessment based on trends and abrupt changes in rainfall characteristics on the Korean peninsula. *Theor. Appl. Climatol.* **2017**, *127*, 305–326. [CrossRef]
47. Cheng, L.; Ma, L.; Yang, M.; Wan, G.; Wang, X. Changes of temperature and precipitation and their impacts on runoff in the upper Taohe River in northwest China from 1956 to 2014. *Environ. Earth Sci.* **2019**, *78*, 423. [CrossRef]
48. Zhang, X.; Dong, Q.; Cheng, L.; Xia, J. A Budyko-based framework for quantifying the impacts of aridity index and other factors on annual runoff. *J. Hydrol.* **2019**, *579*, 124224. [CrossRef]
49. Gao, G.; Fu, B.; Wang, S.; Liang, W.; Jiang, X. Determining the hydrological responses to climate variability and land use/cover change in the Loess Plateau with the Budyko framework. *Sci. Total Environ.* **2016**, *557–558*, 331–342. [CrossRef]

50. Li, Y.; Liu, C.; Yu, W.; Tian, D.; Bai, P. Response of streamflow to environmental changes: A Budyko-type analysis based on 144 river basins over China. *Sci. Total Environ.* **2019**, *664*, 824–833. [CrossRef] [PubMed]
51. Gan, G.; Liu, Y.; Sun, G. Understanding interactions among climate, water, and vegetation with the Budyko framework. *Earth-Sci. Rev.* **2021**, *212*, 103451. [CrossRef]
52. Tan, X.; Liu, B.; Tan, X.; Chen, X. Long-Term Water Imbalances of Watersheds Resulting from Biases in Hydroclimatic Data Sets for Water Budget Analyses. *Water Resour. Res.* **2022**, *58*, e2021WR031209W. [CrossRef]

Disclaimer/Publisher's Note: The statements, opinions and data contained in all publications are solely those of the individual author(s) and contributor(s) and not of MDPI and/or the editor(s). MDPI and/or the editor(s) disclaim responsibility for any injury to people or property resulting from any ideas, methods, instructions or products referred to in the content.